HHS Public Access

Author manuscript

Cell Rep. Author manuscript; available in PMC 2020 November 04.

Published in final edited form as:

Cell Rep. 2020 September 08; 32(10): 108121. doi:10.1016/j.celrep.2020.108121.

No Evidence that Wnt Ligands Are Required for Planar Cell Polarity in *Drosophila*

Ben Ewen-Campen[1], **Typhaine Comyn**[1,3], **Eric Vogt**[1], **Norbert Perrimon**[1,2,4,*]

[1]Department of Genetics, Blavatnik Institute, Harvard Medical School, Boston, MA 02115, USA

[2]Howard Hughes Medical Institute, Boston, MA 02115, USA

[3]Present address: Energy & Memory, Brain Plasticity Unit, Centre National de la Recherche Scientifique, ESPCI, Paris, France

[4]Lead Contact

SUMMARY

The *frizzled* (*fz*) and *dishevelled* (*dsh*) genes are highly conserved members of both the planar cell polarity (PCP) pathway and the Wnt signaling pathway. Given these dual functions, several studies have examined whether Wnt ligands provide a tissue-scale orientation cue for PCP establishment during development, and these studies have reached differing conclusions. Here, we re-examine this issue in the *Drosophila melanogaster* wing and notum using split-Gal4 co-expression analysis, multiplex somatic CRISPR, and double RNAi experiments. Pairwise loss-of-function experiments targeting *wg* together with other Wnt genes, via somatic CRISPR or RNAi, do not produce PCP defects in the wing or notum. In addition, somatic CRISPR against *evi* (aka *wntless*), which is required for the secretion of Wnt ligands, did not produce detectable PCP phenotypes. Altogether, our results do not support the hypothesis that Wnt ligands contribute to PCP signaling in the *Drosophila* wing or notum.

Graphical Abstract

*Correspondence: perrimon@genetics.med.harvard.edu.

AUTHOR CONTRIBUTIONS

B.E.-C. designed and performed experiments, generated reagents, and wrote the manuscript. T.C. performed gut imaging experiments. E.V. generated reagents. N.P. designed experiments and edited the manuscript.

SUPPLEMENTAL INFORMATION

Supplemental Information can be found online at https://doi.org/10.1016/j.celrep.2020.108121.

DECLARATION OF INTERESTS

The authors declare no competing interests.

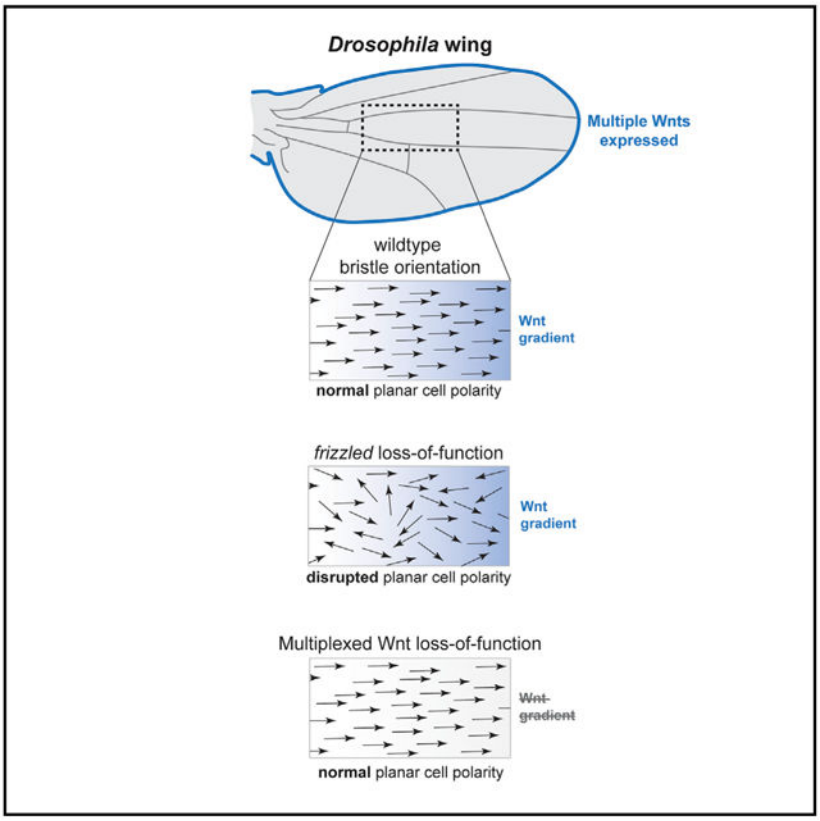

In Brief

Previous studies have come to differing conclusions on whether Wnt ligands provide a tissue-level orientation cue for the planar cell polarity pathway. Ewen-Campen et al. re-examine this question in *Drosophila* using multiplex *in vivo* CRISPR and double RNAi against Wnt ligands and find no evidence that Wnts are required for PCP patterning.

INTRODUCTION

Planar cell polarity (PCP) refers to the coherent orientation of cells in a sheet and is driven by a conserved molecular pathway that is required for the proper development and function of many animal tissues (Adler, 2012; Butler and Wallingford, 2017; Goodrich and Strutt, 2011; Yang and Mlodzik, 2015). Decades of functional analyses in the epithelia of *Drosophila* and other model organisms have led to the identification of six highly conserved "core" pathway members, whose asymmetric localization and function drives downstream manifestations of PCP, both autonomously and non-autonomously. In cells of the developing fruit fly wing, the transmembrane protein Frizzled (Fz) and the cytosolic proteins Dishevelled (Dsh) and Diego (Dgo) accumulate at the distal cortex. At the proximal cortex, an asymmetric signaling complex forms that includes the transmembrane protein Strabismus aka Van Gogh (Stbm/Vang) and the cytosolic protein Prickle (pk). The sixth core pathway member, Flamingo aka Starry night (Fmi/Stan), accumulates both proximally and distally (Adler, 2012; Butler and Wallingford, 2017; Goodrich and Strutt, 2011; Yang and Mlodzik,

2015). Loss of function of any core pathway members leads to PCP defects, which ultimately manifest in mispolarization of the actin-rich wing hairs (Gubb and García-Bellido, 1982; Wong and Adler, 1993). In addition to the core pathway, a second PCP pathway that includes Fat, Dachsous, and Four-jointed has been identified in *Drosophila* (Adler, 2012; Butler and Wallingford, 2017; Goodrich and Strutt, 2011; Yang and Mlodzik, 2015).

At relatively small spatial scales, feedback interactions among core PCP pathway components provide a working molecular model for PCP within cells and between neighboring cells. However, there remains active debate regarding the molecular mechanisms that allow core pathway members to correctly orient regarding "global" patterning at the level of whole tissues. Researchers have long hypothesized that there may be a secreted molecule (referred to as "Factor X" by Lawrence et al., 2002) that coordinates tissue-scale morphogenesis to the PCP pathway. Among the possible candidates for "Factor X," Wnt ligands have long been considered "obvious candidates for such factors" (Goodrich and Strutt, 2011) because both Fz and Dsh are highly conserved members of this signaling pathway: Fz and its paralog Fz2 function as co-receptors for Wnt ligands (Bhanot et al., 1999; Chen and Struhl, 1999; Müller et al., 1999), and Dsh is also a highly conserved component of the Wnt ligand-receptor signalosome (Perrimon and Mahowald, 1987; Sharma et al., 2018). However, a number of loss-of-function studies of Wnt ligands have failed to find any PCP phenotypes (Chen et al., 2008; Lawrence et al., 2002). Specifically, Lawrence et al. (2002) examined clones in the adult abdominal epithelium homozygous for a deletion covering four of the seven *Drosophila* Wnt ligands (*wg, wnt4, wnt6*, and *wnt10*), and found no PCP defects within or nearby such clones. Chen et al., (2008) generated quintuple clones in the wing lacking *wg, wnt2, wnt4, wnt6*, and *wnt10*, as well as clones lacking *porcupine*, a gene necessary for the correct lipid modification of Wnt ligands, and found no evidence of PCP defects in either case. In addition, homozygous mutants for *evi* (aka *wntless*), which are defective in Wnt secretion, display wild-type PCP (Bartscherer et al., 2006)

Because Wg is required in early larval stages to specify the presumptive wing (Ng et al., 1996), the above studies relied on the analysis of *wg* mutant clones in an otherwise wild-type background and thus could not conclusively rule out a role for long-range Wnt signaling from surrounding cells. In contrast, some gain-of-function studies have demonstrated that overexpression of either Wg or Wnt4 (but not other Wnt ligands) in ectopic regions of the developing wing can reorient the polarity of surrounding wing hairs (Lim et al., 2005; Wu et al., 2013) and that this reorientation requires *fz* (Wu et al., 2013), although a study in the abdomen did not see re-polarization when overexpressing the seven Wnt ligands in a *dachsous* $-/-$ background (Casal et al., 2006). In addition, a study that bypassed the early requirements for *wg* using a temperature-sensitive mutation indicated that double-mutant flies lacking *wg* and *wnt4* displayed statistically significant PCP phenotypes in the pupal and adult wing (Wu et al., 2013). Furthermore, studies in vertebrates have implicated certain Wnt ligands in PCP signaling (Yang and Mlodzik, 2015). Taken together, the evidence on whether Wnts, either individually or in combination, influence PCP signaling remains inconclusive.

In this study, we re-examine whether Wnt ligands are required for PCP using systematic double and triple CRISPR via Gal4-UAS-driven Cas9 and double RNAi. We independently analyzed the expression of each Wnt using a collection of knockin split-Gal4 reporters and performed multiplex somatic CRISPR using short guide RNAs (sgRNAs) targeting *wg* in combination with each of the other six Wnt genes, as well as various combinations thereof. In addition, we used somatic CRISPR to target *evi* (*wntless*), a protein required for the secretion of Wnt genes except *wntD* (Herr and Basler, 2012). Last, we performed double RNAi experiments against *wg, wnt4*, and *wnt6* in the wing and in the notum. We did not detect PCP phenotypes in any of these loss-of-function conditions, in either wing or notum. In contrast to previous reports, our results do not support the hypothesis that Wnt ligands impinge on PCP signaling. We note that our data are consistent with a study recently posted on bioRxiv (Yu et al., 2020), which we discuss below.

RESULTS

Split-Gal4 Knockin Reporters Confirm that Multiple Wnt Genes Are Co-expressed in the Larval Wing Disc

To characterize which Wnt genes are expressed in the wing disc during the period when PCP patterning is established in the developing wing, we systematically re-examined the expression and co-expression of the seven *Drosophila* Wnt family genes. In the wing disc, core PCP components progressively acquire asymmetrically localization during pupal stages, and there is also evidence that at least some polarity information exists during L3 larval stages in the form of coherent Fmi/Stan localization that is subsequently remodeled during pupal stages (Classen et al., 2005). To independently examine which Wnt ligands are expressed during wing development, we used CRISPR-based homology directed repair to knock in split-Gal4 reporter cassettes into an early exon of each Wnt gene (Figure 1A) (Gratz et al., 2014; Pfeiffer et al., 2010). These cassettes include an in-frame T2A self-cleaving peptide, followed by either the p65 activation domain or the Gal4 DNA binding domain (DBD), and thus allow intersectional labeling of cells expressing multiple Wnt genes. Pilot experiments with *wg* and *wnt2* indicated that this approach recapitulates previously described endogenous gene expression of *wg* and *wnt2*, for both p65 and Gal4DBD knockins (Figure S1) (Chen et al., 2008; Kozopas and Nusse, 2002). As predicted, homozygous *wg* knockins were lethal, and *wnt2* knockin homozygotes were male sterile and displayed characteristic wing posture abnormalities (Kozopas and Nusse, 2002; Kozopas et al., 1998). We ultimately created split-Gal4 knockin reagents for each of the seven Wnt genes. In support of the accuracy and utility of these split-Gal4 reporters, we find that they recapitulate known Wnt expression in the adult ovary and that they can be used to characterize Wnt-expressing cells various adult stem cell populations of the gut, and in the larval CNS, which we summarize below.

We crossed this collection of split-Gal4 reagents to a ubiquitously expressed cognate (Gal4DBD or VP16 driven by the *tubulin* promoter) and examined the expression in larval wing discs via a UAS-driven fluorophore (Figure 1A). We observed expression of *wg, wnt2*, and *wnt6* in the L3 wing disc, consistent with previous reports (Baker, 1988; Janson et al., 2001; Kozopas and Nusse, 2002). Split-Gal4 intersection analysis confirmed that *wg* and

wnt2 are co-expressed in the epithelium of the developing notum and a portion of the wing pouch, and that *wg* and *wnt6* are extensively co-expressed throughout their entire expression domain at this stage (Janson et al., 2001) (Figure 1B). In the pupal wing margin, we observed overlapping expression of *wg, wnt2, wnt4*, and *wnt6* (Figure 1C).

Unexpectedly, although we did observe *wnt4* expression in the margin of the pupal wing (Figures 1D and S2), we did not detect *wnt4* expression in the dorsoventral (DV) boundary at the L3 larval stage, as has been demonstrated via RNA *in situ* hybridization (Chen et al., 2008; Gieseler et al., 2001; Harris et al., 2016) and a GFP knockin (Yu et al., 2020). Instead, our *wnt4* reporter drove UAS:GFP expression in a small cluster of cells at the anterior ventral boundary of the wing pouch and was not detected in the wing margin until early pupal stages (Figures 1B and S2). Given this discrepancy between our reporter line and previous studies, we examined the expression pattern of an existing knockin Gal4 reporter from the CRIMIC collection, which contains a "trojan exon" including a splice acceptor and T2A-Gal4, inserted in the first intron of *wnt4* (Lee et al., 2018). The expression of $wnt4^{CRIMIC}$ was consistent with our split-Gal4 reporter in the L3 wing disc and largely consistent in the larval CNS (Figure S2). As an additional test, we generated a third knockin reporter (using T2A-Gal4) using an independently derived donor plasmid (Bosch et al., 2020), inserted into the final exon of *wnt4*. This independent Gal4 insertion ($wnt4^{T2A\text{-}Gal4}$) was consistent with the other two tested in this study and did not show detectable expression in the DV boundary at the L3 stage (Figure S2). To test whether *wnt4* may be expressed in the wing disc during earlier stages, we crossed $wnt4^{CRIMIC}$ line to G-TRACE, a lineage-tracing tool that reports both current and past Gal4 expression using two different fluorophores (Evans et al., 2009). This analysis did not reveal any past expression in the wing disc aside from the small cluster of cells on the border of the wing pouch. Using RNA *in situ* hybridization, we found that Gal4 is transcribed in the DV boundary at the L3 stage in *wnt4-T2A-Gal4* flies, suggesting that the Gal4-UAS system introduces a temporal delay in GFP expression relative to endogenous *wnt4* expression.

To provide additional validation of the split-Gal4 lines described in this study, we examined Wnt ligand expression in the adult ovary, larval CNS, and two stem cell populations in the adult gut (Figures S3 and S4). In the adult ovary, our split-Gal4 for *wg, wnt2, wnt4*, and *wnt6* are co-expressed in a partially overlapping pattern in the female germarium, consistent with previous descriptions (Waghmare and Page-McCaw, 2018). In addition, we found that *wnt5* is also expressed in the adult germarium, in a pattern similar to *wnt6* (Figure S3A), which to our knowledge has not been previously reported.

In the adult gut, we find that *wg, wnt2, wnt4*, and *wnt6* are co-expressed in and surrounding adult stem cells located in the cardia (located at the foregut-midgut junction) and, with the exception of *wnt2*, at the midgut-hindgut juncture (Figure S4) (Singh et al., 2011; Tian et al., 2016). These observations add to our understanding of which ligands are responsible for Wnt signaling observed in these regions of the gut (Tian et al., 2016, 2018) and support the observation that overlapping expression of multiple Wnt ligands is a common feature of different adult stem cell populations in *Drosophila*.

We also examined Wnt gene expression in the larval nervous system. *wg, wnt4*, and *wnt5* are known to have roles in the developing nervous system (Inaki et al., 2007; Packard et al., 2002; Yoshikawa et al., 2003), and we find that in fact all Wnts are expressed in the larval nervous system. This includes *wnt10* (Figure S4). Thus, these split-Gal4 lines may be useful for future studies of Wnt function and redundancy.

Systematic Pairwise CRISPR against Wnt Genes Using Gal4-UAS:Cas9

Previous studies in *Drosophila* have demonstrated that ectopic expression of either Wg or Wnt4 can reorient PCP patterning in surrounding wing hairs (Lim et al., 2005; Wu et al., 2013), and Wu et al. (2013) reported that double mutants for *wg* and *wnt4* display disrupted PCP signaling in the pupal and adult wing. We sought to systematically address the role of Wnt ligands in PCP signaling using multiplexed *in vivo* somatic CRISPR. For these experiments, we identified two effective sgRNAs to target each Wnt ligand (see STAR Methods) and created transgenic lines expressing sgRNAs targeting either one or two Wnt genes simultaneously (with either two or four sgRNAs total, respectively) under UAS control. We confirmed that these sgRNAs cleaved their intended target *in vivo* both for single- and double-targeting experiments (Figure S5).

To avoid early roles for Wg in wing specification, we used the *nubbin*-Gal4 driver to express both Cas9 and sgRNAs. *nubbin*-Gal4 is expressed throughout the wing pouch beginning in late L2 larval stages (Zirin and Mann, 2007), and thus this approach allowed us to permanently remove target gene function throughout L3, pupal, and adult stages. Control experiments targeting *fz* confirmed that this approach produces strong PCP phenotypes in the adult wing (Figure 2; Figure S6) and that *frizzled* is unique among the four Fz-family genes in producing this phenotype, both in single and pairwise CRISPR experiments (Figure S6). Although we did not detect expression of reporters for *wnt5, wntD*, or *wnt10* in the wing disc, we included them in our functional studies in order to rule out the possibility that one or more of these ligands is expressed at low levels.

We used somatic CRISPR to target *wg* together with *wnt4*, as well as each of the other five Wnt genes and screened for defects in both wing morphology and PCP. As expected, the wing margin was disrupted in all pairwise CRISPR experiments that included *wg*, and the intervein regions were reduced in size (Figure 2). However, in each case, wing hair orientation was indistinguishable from wild-type (compare with *fz* panel in Figure 1 and Figure S6 for examples of PCP phenotypes caused by disrupting *fz*). We next tested pairwise combinations of *wnt4, wnt6*, and *wnt10*, which are part of a genomic cluster on the second chromosome, as well as triple CRISPR against *wg, wnt4*, and *wnt6*, and against *wg, wnt2*, and *wnt4*. We did not observe disrupted PCP in any of these conditions (Figure 2). Last, we used this approach to target *evi* (*wntless*), which is required for the secretion of all Wnt genes except WntD (Bänziger et al., 2006; Bartscherer et al., 2006; Goodman et al., 2006; Herr and Basler, 2012). Knocking out *evi* led to loss of wing margin, essentially phenocopying *wg* loss of function, and did not produce PCP defects, consistent with observations from *evi* mutant pharate adults (Bartscherer et al., 2006) (Figure 2). Together, these results suggest that Wg and Wnt4 are not redundantly involved in global PCP

patterning and provide no evidence that Wnt ligands direct PCP orientation in the *Drosophila* wing.

Pairwise RNAi against *wg* Together with *wnt4* or *wnt6* Does Not Produce PCP Phenotypes in the Wing or Notum

Somatic Gal4-UAS-based CRISPR has been shown to be a powerful and scalable technique for *in vivo* knockouts (Port and Bullock, 2016; Port et al., 2020). However, one inherent drawback of somatic CRISPR is that it creates mosaic tissues containing both mutant and wild-type cells and does so variably between individuals. This can be seen, for example, in the variable phenotypes and incomplete loss of margin tissue observed when targeting *wg* (Figure 2). In the case of morphogens such as Wnt ligands, it is conceivable that a small number of wild-type cells could still be sufficient to produce an instructive cue for PCP orientation.

To address this issue, we performed double RNAi experiments against *wg, wnt4*, and *wnt6* in the developing wing using *nub*-Gal4, using transgenic double-stranded RNA (dsRNA) lines recently shown to produce strong loss-of-function phenotypes and co-expressed with UAS:*dcr2* to strengthen RNAi-mediated knockdown (Barrio and Milán, 2020). Under these conditions, *wg* RNAi led to both a complete loss of the wing margin and a profound growth defect, similar in appearance to the effects of inducing apoptosis in *wg*-expressing cells by overexpressing the pro-apoptotic genes *hid* and *rpr* (Yu et al., 2020). However, even in these severely mispatterned wings, PCP appeared wild-type. Similarly, no PCP defects were observed upon pairwise RNAi against *wg* and *wnt4* or *wg* and *wnt6* (Figure 3). Incidentally, our results confirmed recent observations that *wnt4* and *wnt6* have opposing effects on modulating the effects of *wg*-dependent growth (Barrio and Milán, 2020).

Fz-dependent PCP phenotypes can also be studied in the adult notum, by the orientation of bristles (Figure S7A). We thus used pairwise RNAi to knock down *wg* and *wnt4* or *wg* and *wnt6* in the adult notum using *pnr*-Gal4. Consistent with our observations in the adult wing, we observed no discernable PCP phenotypes in the adult notum in any of these conditions (Figure S7).

DISCUSSION

In this study, we performed loss-of-function studies in the wing and notum using multiplexed somatic CRISPR and double RNAi to systematically target Wnt ligands, and in no combination did we observe PCP phenotypes. In contrast to a study that found a role for Wg and Wnt4 in global PCP establishment (Wu et al., 2013), our results provide no evidence that Wnt ligands, whether singly or redundantly with one another, necessary to provide an instructive global cue to the core PCP pathway. If there is a secreted “Factor X” molecule that provides tissue-scale information, our results suggest that it is not a Wnt ligand or combination of two or three Wnt ligands. Previous experiments have suggested that this hypothetical factor is not a member of the Notch, EGF, FGF, or Dpp signaling pathways (Lawrence et al., 2002).

Our results do not rule out the possibility that Wnt ligands could play a redundant role with an additional global cue or cues. For example, a number of studies have suggested that signaling via Fat, Dachsous, and Four-jointed may provide large-scale positional information that is interpreted and refined by the activity of core PCP components within and between neighboring cells (Butler and Wallingford, 2017; Goodrich and Strutt, 2011). The mechanisms that couple local and global PCP thus remain incompletely understood.

Our results imply that the ability of ectopically expressed Wg and Wnt4 to reorient the PCP of surrounding cells is not reflective of such a role in wild-type flies. One possible explanation for these results is that feedback mechanisms between Wnt ligands and Fz proteins may account for the ability of ectopic Wnt ligands to disrupt wild-type Fz function (Cadigan et al., 1998; Chaudhary et al., 2019), irrespective of the physiological role for Wnts under normal conditions. We also note that a separate study found that overexpression of any of the seven UAS:Wnt ligands in clones in the adult abdomen did not cause bristle reorientation (Casal et al., 2006).

During the preparation of this manuscript, a preprint by Yu et al. (2020) reported related data and similar conclusions using several independent approaches. Specifically, Yu et al. (2020) found that normal PCP patterning occurs in the wings of double-mutant flies expressing only membrane-tethered Wg and homozygous for mutations for *wnt4*, as well as in quintuple mutant lacking *wnt2, wnt4, wnt6*, and *wnt10* and expressing solely membrane-tethered Wg. They also report that *evi/wntless* loss of function does not interfere with PCP, nor does driving apoptosis in all *wg*-expressing cells in the developing disc by overexpressing *hid* and *rpr*.

One experimental difference between our studies and those reported by Yu et al. (2020) is that the latter use a membrane-tethered Wg mutant, rather than a knockout or knockdown approach, when addressing Wg function. These mutants lack secreted Wg yet, unlike *wg* loss-of-function mutants, display nearly normal patterning and development (Alexandre et al., 2014). Subsequent studies have attributed this phenomenon to a combination of *fz2*-dependent feedback and perdurance of membrane-tethered Wg from earlier stages (Chaudhary et al., 2019). Thus, it is formally possible that membrane-tethered Wg could serve as a global PCP cue in these experiments, even if not secreted. In the present study, we use both somatic CRISPR and RNAi to greatly reduce or eliminate *wg* function altogether. We note, for example, that our *wg* RNAi phenotypes resemble those caused by inducing apoptosis in *wg*-expressing cells and thus likely represent very strong loss-of-function phenotypes, yet we also observed no PCP phenotypes. Taken together, the results presented in the present study are complementary and consistent with those presented by Yu et al. (2020): both studies fail to confirm the hypothesis that Wg and Wnt4 are redundantly required for global PCP orientation in the *Drosophila* wing, and both studies provide accumulate additional evidence that Wnt ligands in general, whether singly or jointly, are not required for PCP orientation in the *Drosophila* wing in an otherwise wild-type background.

A Note on Somatic CRISPR versus RNAi

A number of studies have demonstrated that *in vivo* somatic CRISPR is an effective and scalable approach for loss-of-function studies (Poe et al., 2019; Port and Bullock, 2016; Port et al., 2020), and the results in the present study further demonstrate that this approach can also be applied to efficiently perform multiplexed somatic knockouts in a tissue-specific manner. Our results also illustrate a known caveat of the approach that may be especially relevant for secreted factors: somatic CRISPR leads to mosaic tissues that contain a mixture of wild-type and mutant cells. Although the proportion of mutant cells can be increased by using multiple sgRNAs (Port and Bullock, 2016), it is unlikely to ever reach 100%, and variability between individuals is likely to remain an issue. For secreted proteins such as Wg, even small numbers of remaining cells that secrete wild-type protein may affect the interpretation of results. *In vivo* RNAi, on the other hand, tends to be far more uniform within and between individuals, and in those cases in which particularly effective reagents are available, such as those used in the present study (compare *wg* loss-of-function phenotypes in Figures 2 and 3), this can result in stronger tissue-level phenotypes than somatic CRISPR. Thus, the advent of somatic CRISPR does not obviate the power of *in vivo* RNAi for functional studies.

STAR★METHODS

RESOURCE AVAILABILITY

Lead Contact—Further information and requests for resources and reagents should be directed to and will be fulfilled by the Lead Contact, Norbert Perrimon (perrimon@genetics.med.harvard.edu)

Materials Availability—All unique/stable reagents generated in this study are available from the Lead Contact without restriction.

Data and Code Availability—This study did not generate any unique datasets or code.

EXPERIMENTAL MODEL AND SUBJECT DETAILS

Fly strains—*Drosophila melanogaster* stocks were maintained and crossed on standard laboratory cornmeal food, and all experiments were conducted at 25°C. The following previously described stocks were used: *nub-Gal4 ; UAS:Cas9.P2* (BL67086), *UAS:dcr2 ; nub-Gal4* (BL25754), *pnr-Gal4 / TM3* (Perrimon lab stock), *elav-Gal4 ; UAS:Cas9.P2* (BL67073), split-Gal4 “p65 tester line”: *tub::Gal4DBD, UAS:EGFP* (BL60298), split-gal4 “Gal4DBD tester line*”: tub::VP16[AD], UAS:EYFP* (BL60294), *wnt4* CRIMIC “trojan Gal4” (BL67449), GTRACE: *UAS-RedStinger, UAS-Flp1.D, Ubi (FRT.Stop)Stinger/CyO* (BL28280), GFP RNAi: HMS00314 (Perrimon lab stock), *pCFD6-wntless*^{2X} – gift of F. Port (Port and Bullock, 2016), *wg* RNAi – dsRNA, VDRC (KK104579), *wnt4* RNAi – dsRNA, VALIUM10 vector (BL29442), *wnt6* RNAi – dsRNA, VDRC (GD26669), UAS:2xEGFP (BL60293)

***Drosophila* cell lines—**Cas9-expressing S2R+ cell lines, used to estimate sgRNA efficiency, are described in Viswanatha et al. (2018).

METHOD DETAILS

sgRNAs construction—For each Wnt ligand, five candidate sgRNAs were designed using the *Drosophila Resource Screening Center Find CRISPRv2* online tool (https://www.flyrnai.org/crispr2/). These five candidate sgRNAs were cloned into U6:3-expression vector pCFD3 (Port et al., 2014), and tested for cutting efficiency in S2R+ cells engineered to express Cas9 (Viswanatha et al., 2018), followed by T7 endonuclease activity three days after transfection. Cutting efficiency was estimated by quantifying band intensity via ImageJ, and the top two scoring sgRNAs were selected for usage in this study. *In vivo* guides were cloned into pCFD6, which expresses multiple sgRNAs under UASt control, each flanked by tRNA sequences (Port and Bullock, 2016). The sgRNA sequences used in this study are shown in Table S1. For single gene knock-out experiments, two sgRNAs were cloned into the pCFD6 backbone and inserted into the attP2 landing site on the third chromosome, and for double gene knock-out experiments, four sgRNAs were cloned into pCFD6, two sgRNAs per target gene, and inserted into the attP40 site on the second chromosome, using standard PhiC31 recombination. For triple-CRISPR experiments, single-target sgRNA constructs on the third chromosome (attP2) were combined with double-target sgRNA constructs on the second chromosome (attP40) using genetic crosses.

Construction of pCFD4^{FLPOUT} vector (used in Figure S6)—For pairwise *frizzled* knock-out experiments, we created a modified pCFD4 variant (Port et al., 2014) conceptually based on the Co-inFLP approach described in Bosch et al. (2015). In this two-guide sgRNA vector, each sgRNA is flanked by a distinct fluorescent reporter, and interlocking FRT/FRT3 sites, for a final orientation of *FRT-3xP3-GFP-U6:1-sgRNA1-FRT3-FRT-U6:3-sgRNA2-3xP3-mCherry-FRT3*. This fragment was synthesized by GENEWIZ, Inc. (South Plainfield, NJ) and subcloned into the pCFD4 backbone using Gibson cloning.

We reasoned that this plasmid would allow us to create a single transgenic fiy line expressing two guides, and to subsequently generate each of the two single sgRNA components by crossing this “parent” line to a source of *hsFlp* and screening the offspring for those that underwent each of the two possible recombination events (FRT versus FRT3), which would express either GFP and mCherry. We validated that this construct successfully expressed two sgRNAs targeting *ebony* and *forked*, which both produce visible adult phenotypes (not shown). We also validated that the FLP-FRT procedure could be used to successfully generate two stable single-sgRNA lines from one “parent” double-sgRNA line. This construct may be of interest for those wishing to screen large numbers of pairs of genes, and subsequently perform single gene studies on a smaller subset of those genes.

T7 endonuclease assay—To test for *in vivo* target cleavage of Wnt genes, pCFD6 males were crossed to unmated *elav-Gal4; UAS:Cas9.P2* females, and the adult heads of their F1 offspring were collected for genomic DNA. ~5-10 heads were collected on dry ice and genomic DNA was extracted by physical homogenization in DNA extraction buffer (10mM Tris-Cl pH 8.2, 1mM EDTA, 25mM NaCL, 200 μg/mL Proteinase K), followed by incubation at 37°C for 20-30 minutes, then boiling at 98°C for ~90 s to inactivate Proteinase K. 1 μL of genomic DNA was used as template in a 20 μL PCR reaction using primers described in Table S2 to amplify regions surrounding the sgRNA target site. PCP products

were used as template for T7 endonuclease assay (New England BioLabs), following manufacturer instructions, and digested products were visualized on a 2% agarose gel.

Generation of split-Gal4 knock-in reporter lines—To create split-Gal4 donor vectors (both p65 and Gal4DBD), p65 and Gal4DBD amplified from pBPp65ADZpUw (Addgene 26234) and pBPZpGAL4DBDUw (Addgene 26233), respectively, and subcloned into pHD-dsRed-attP (Addgene 51019) (Gratz et al., 2014; Pfeiffer et al., 2010). For each Wnt gene, homology arms of approximately 1 kb flanking the sgRNA were designed to create an in-frame fusion between the first exon of the target gene and the T2A sequence of the donor construct, and were cloned into donor vector using Gibson cloning.

Donor constructs and sgRNAs (in pCFD3) were co-injected into *yv ;; nanos:Cas9* flies. Injected offspring were backcrossed to balancer stocks on the X, II, or III chromosome depending on the target gene, and screened for RFP+ eyes. Multiple transformants were recovered for both p65 and Gal4DBD knock-ins of each Wnt gene, with the exception of *wnt4* and *wnt10*, for which only p65 and Gal4DBD lines were recovered, respectively. Expression patterns were ascertained by crossing to ubiquitous split-Gal4 "tester lines" (BL60298 and BL60294), which ubiquitously express either VP16 or Gal4DBD together with a UAS-driven reporter. For every Wnt-family knock-in created, multiple transformants gave indistinguishable expression patterns, regardless of whether p65 or Gal4DBD was knocked-in. PCR analyses confirmed that each line was inserted in the predicted location, with the exception of *wntD*, which we were unable to conclusively validate via PCR. We note that all *wntD* knock-in lines, independently generated, and both with p65 and Gal4DBD, recapitulate indistinguishable expression patterns from one another.

Generation of additional Wnt4 reporter lines—An additional *wnt4* reporter line was generated using a "universal donor" homology-independent knock-in strategy (Bosch et al., 2020). Briefly, a universal T2A-Gal4, 3xP3-dsRed donor was injected into *yv* ;; *nos::Cas9* embryos along with two sgRNAs: one to linearize the donor construct and one to target in the last exon of *wnt4*. These injected flies were crossed to a *w ; Sp/CyO ; UAS-GFP* balancer line and screened for RFP and GFP expression. Of 28 fertile injected flies, six were RFP+, of which five failed to drive UAS::GFPexpression, indicating they were likely out-of-frame and/or inserted at the wrong location. The remaining one RFP+ line drove UAS:GFP in an expression pattern indistinguishable from the two other *wnt4* lines tested in this study.

Antibody staining and imaging—Tissues were dissected in cold PBS, fixed for 20-30 minutes in 4% paraformaldehyde in PBS, and then stained following standard immunhistochemical protocols. Tissues were stained with rabbit anti-GFP conjugated to Alexa 488 (Molecular Probes, 1:400) and DAPI (1:1000), and imaged using either a Zeiss LSM 780 or an Olympus IX83 confocal microscope, both part of the Microscopy Resources of the North Quad (MicRoN) facility at Harvard Medical School. Maximum intensity projections are shown for all tissues except the proventriculus, for which single z-slices are also shown. Adult wings were mounted in a 1:1 mixture of Permount (Fisher) and xylenes, and imaged using brightfield optics on a Zeiss Axioskop 2. Nota were imaged using a Zeiss AxioZoom, and z stacks were compiled into a single image using Helicon Focus software.

***In situ* hybridization—**RNA probes against *wnt4* and *Gal4* were generated by amplifying T7-containing PCR fragments using primers shown in Table S2, which contain 5′ and 3′ linker sequences that allow directional T7 sites to be added in a second PCR reaction, for either antisense or sense probe synthesis. Digoxigenin-labeled RNA probes were synthesized and purified using T7 5X Megascript kit (Invitrogen). L3 larvae were bisected, inverted, and fixed overnight in 4% paraformaldehyde, then sequentially dehydrated into methanol, stored at −20°C for three days, washed twice with ethanol, treated with 1:1 ethanol:xylenesforone hour, then rehydrated, washed repeatedly with PBS + 0.3% Triton-X, and hybridized overnight at 58°C with RNA probes at 100 ng/μL in RNA hybridization buffer (50% formamide, 5X SSC, 0.1mg/mL heparin, 1.0% salmon sperm single stranded DNA, 0.1% Tween-20 in RNase-free water.) Larvae were then washed repeatedly in hybridization buffer, a series of increasingly dilute hybridization buffer, multiple washes of PBS + 0.3% Trixon-X, and incubated overnight with anti-digoxigenin-AP Fab fragments (Roche, 1:1000). Finally, larvae were washed repeatedly with PBS + 0.3% Triton-X, and signal was detected using 5-bromo-4-chloro-3-indolyl-phosphate/nitro blue tetrazolium (Promega) following manufacturer's protocol, then washed in ethanol, mounted in vectashield, and imaged using brightfield optics on a Zeiss Axioskop 2.

QUANTIFICATION AND STATISTICAL ANALYSIS

This study did not use quantification or statistical analysis.

Supplementary Material

Refer to Web version on PubMed Central for supplementary material.

ACKNOWLEDGMENTS

We thank Fillip Port for providing pCFD6-*evi* flies; Marco Milan and Lara Barrios for providing combined RNAi lines targeting *wg, wnt4*, and *wnt6*; Rich Binari for assistance with fly work; Justin Bosch for assistance designing pCFD4^{FLPOUT}; and Pedro Saavedra, Stephanie Mohr, Sudhir Tattikota, and members of the Perrimon lab for critical feedback. B.E.-C. received funding from the Charles A. King Postdoctoral Research Fellowship program, and the Perrimon lab received funding from NIH Office of Research Infrastructure Programs (ORIP) grant R24 OD26435 and the Howard Hughes Medical Institute (HHMI).

REFERENCES

Adler PN (2012). The frizzled/stan pathway and planar cell polarity in the Drosophila wing. Curr. Top. Dev. Biol 101, 1–31. [PubMed: 23140623]

Alexandre C, Baena-Lopez A, and Vincent J-P (2014). Patterning and growth control by membrane-tethered Wingless. Nature 505, 180–185. [PubMed: 24390349]

Baker NE (1988). Transcription of the segment-polarity gene wingless in the imaginal discs of Drosophila, and the phenotype ofapupal-lethal wg mutation. Development 102, 489–497. [PubMed: 3181031]

Bänziger C, Soldini D, Schütt C, Zipperlen P, Hausmann G, and Basler K (2006). Wntless, a conserved membrane protein dedicated to the secretion of Wnt proteins from signaling cells. Cell 125, 509–522. [PubMed: 16678095]

Barrio L, and Milán M (2020). Regulation of anisotropic tissue growth by two orthogonal signaling centers. Dev. Cell 52, 659–672.e3. [PubMed: 32084357]

Bartscherer K, Pelte N, Ingelfinger D, and Boutros M (2006). Secretion of Wnt ligands requires Evi, a conserved transmembrane protein. Cell 125, 523–533. [PubMed: 16678096]

Bhanot P, Fish M, Jemison JA, Nusse R, Nathans J, and Cadigan KM (1999). Frizzled and Dfrizzled-2 function as redundant receptors for Wingless during Drosophila embryonic development. Development 126, 4175–4186. [PubMed: 10457026]

Bosch JA, Tran NH, and Hariharan IK (2015). CoinFLP: a system for efficient mosaic screening and for visualizing clonal boundaries in Drosophila. Development 142, 597–606. [PubMed: 25605786]

Bosch JA, Colbeth R, Zirin J, and Perrimon N (2020). Gene knock-ins in *Drosophila* using homology-independent insertion of universal donor plasmids. Genetics 214, 75–89. [PubMed: 31685521]

Butler MT, and Wallingford JB (2017). Planar cell polarity in development and disease. Nat. Rev. Mol. Cell Biol 18, 375–388. [PubMed: 28293032]

Cadigan KM, Fish MP, Rulifson EJ, and Nusse R (1998). Wingless repression of Drosophila frizzled 2 expression shapes the Wingless morphogen gradient in the wing. Cell 93, 767–777. [PubMed: 9630221]

Casal J, Lawrence PA, and Struhl G (2006). Two separate molecular systems, Dachsous/Fat and Starry night/Frizzled, act independently to confer planar cell polarity. Development 133, 4561–4572. [PubMed: 17075008]

Chaudhary V, Hingole S, Frei J, Port F, Strutt D, and Boutros M (2019). Robust Wnt signaling is maintained by a Wg protein gradient and Fz2 receptor activity in the developing *Drosophila* wing. Development 146, dev174789. [PubMed: 31399474]

Chen CM, and Struhl G (1999). Wingless transduction by the Frizzled and Frizzled2 proteins of Drosophila. Development 126, 5441–5452. [PubMed: 10556068]

Chen W-S, Antic D, Matis M, Logan CY, Povelones M, Anderson GA, Nusse R, and Axelrod JD (2008). Asymmetric homotypic interactions of the atypical cadherin flamingo mediate intercellular polarity signaling. Cell 133, 1093–1105. [PubMed: 18555784]

Classen A-K, Anderson KI, Marois E, and Eaton S (2005). Hexagonal packing of Drosophila wing epithelial cells by the planar cell polarity pathway. Dev. Cell 9, 805–817. [PubMed: 16326392]

Evans CJ, Olson JM, Ngo KT, Kim E, Lee NE, Kuoy E, Patananan AN, Sitz D, Tran P, Do M-T, et al. (2009). G-TRACE: rapid Gal4-based cell lineage analysis in Drosophila. Nat. Methods 6, 603–605. [PubMed: 19633663]

Gieseler K, Wilder E, Mariol MC, Buratovitch M, Bérenger H, Graba Y, and Pradel J (2001). DWnt4 and wingless elicit similar cellular responses during imaginal development. Dev. Biol 232, 339–350. [PubMed: 11401396]

Goodman RM, Thombre S, Firtina Z, Gray D, Betts D, Roebuck J, Spana EP, and Selva EM (2006). Sprinter: a novel transmembrane protein required for Wg secretion and signaling. Development 133, 4901–4911. [PubMed: 17108000]

Goodrich LV, and Strutt D (2011). Principles of planar polarity in animal development. Development 138, 1877–1892. [PubMed: 21521735]

Gratz SJ, Ukken FP, Rubinstein CD, Thiede G, Donohue LK, Cummings AM, and O'Connor-Giles KM (2014). Highly specific and efficient CRISPR/Cas9-catalyzed homology-directed repair in Drosophila. Genetics 196, 961–971. [PubMed: 24478335]

Gubb D, and García-Bellido A (1982).A genetic analysis of the determination of cuticular polarity during development in Drosophila melanogaster. J. Embryol. Exp. Morphol 68, 37–57. [PubMed: 6809878]

Harris RE, Setiawan L, Saul J, and Hariharan IK (2016). Localized epigenetic silencing of a damage-activated WNT enhancer limits regeneration in mature Drosophila imaginal discs. eLife 5, 49.

Herr P, and Basler K (2012). Porcupine-mediated lipidation is required for Wnt recognition by Wls. Dev. Biol 361, 392–402. [PubMed: 22108505]

Inaki M, Yoshikawa S, Thomas JB, Aburatani H, and Nose A (2007). Wnt4 is a local repulsive cue that determines synaptic target specificity. Curr. Biol 17, 1574–1579. [PubMed: 17764943]

Janson K, Cohen ED, and Wilder EL (2001). Expression of DWnt6, DWnt10, and DFz4 during Drosophila development. Mech. Dev 103, 117–120. [PubMed: 11335117]

Kozopas KM, and Nusse R (2002). Direct flight muscles in Drosophila develop from cells with characteristics of founders and depend on DWnt-2 for their correct patterning. Dev. Biol 243, 312–325. [PubMed: 11884040]

Kozopas KM, Samos CH, and Nusse R (1998). DWnt-2, a Drosophila Wnt gene required for the development of the male reproductive tract, specifies a sexually dimorphic cell fate. Genes Dev. 12, 1155–1165. [PubMed: 9553045]

Lawrence PA, Casal J, and Struhl G (2002). Towards a model of the organisation of planar polarity and pattern in the Drosophila abdomen. Development 129, 2749–2760. [PubMed: 12015301]

Lee P-T, Zirin J, Kanca O, Lin W-W, Schulze KL, Li-Kroeger D, Tao R, Devereaux C, Hu Y, Chung V, et al. (2018). A gene-specific *T2A-GAL4* library for *Drosophila*. eLife 7, e35574. [PubMed: 29565247]

Lim J, Norga KK, Chen Z, and Choi KW (2005). Control of planar cell polarity by interaction of DWnt4 and four-jointed. Genesis 42, 150–161. [PubMed: 15986451]

Müller HA, Samanta R, and Wieschaus E (1999). Wingless signaling in the Drosophila embryo: zygotic requirements and the role of the frizzled genes. Development 126, 577–586. [PubMed: 9876186]

Ng M, Diaz-Benjumea FJ, Vincent JP, Wu J, and Cohen SM (1996). Specification of the wing by localized expression of wingless protein. Nature 381, 316–318. [PubMed: 8692268]

Packard M, Koo ES, Gorczyca M, Sharpe J, Cumberledge S, and Budnik V (2002). The Drosophila Wnt, wingless, provides an essential signal for pre- and postsynaptic differentiation. Cell 111, 319–330. [PubMed: 12419243]

Perrimon N, and Mahowald AP (1987). Multiple functions of segment polarity genes in Drosophila. Dev. Biol 119, 587–600. [PubMed: 3803719]

Pfeiffer BD, Ngo T-TB, Hibbard KL, Murphy C, Jenett A, Truman JW, and Rubin GM (2010). Refinement of tools for targeted gene expression in Drosophila. Genetics 186, 735–755. [PubMed: 20697123]

Poe AR, Wang B, Sapar ML, Ji H, Li K, Onabajo T, Fazliyeva R, Gibbs M, Qiu Y, Hu Y, and Han C (2019). Robust CRISPR/Cas9-mediated tissue-specific mutagenesis reveals gene redundancy and perdurance in *Drosophila*. Genetics 211, 459–472. [PubMed: 30504366]

Port F, and Bullock SL (2016). Augmenting CRISPR applications in Drosophila with tRNA-flanked sgRNAs. Nat. Methods 13, 852–854. [PubMed: 27595403]

Port F, Chen H-M, Lee T, and Bullock SL (2014). Optimized CRISPR/Cas tools for efficient germline and somatic genome engineering in Drosophila. Proc. Natl. Acad. Sci. U S A 111, E2967–E2976. [PubMed: 25002478]

Port F, Strein C, Stricker M, Rauscher B, Heigwer F, Zhou J, Beyersdörffer C, Frei J, Hess A, Kern K, et al. (2020). A large-scale resource for tissue-specific CRISPR mutagenesis in *Drosophila*. eLife 9, e53865. [PubMed: 32053108]

Sharma M, Castro-Piedras I, Simmons GE Jr., and Pruitt K (2018). Dishevelled: a masterful conductor of complex Wnt signals. Cell. Signal 47, 52–64. [PubMed: 29559363]

Singh SR, Zeng X, Zheng Z, and Hou SX (2011). The adult Drosophila gastric and stomach organs are maintained by a multipotent stem cell pool at the foregut/midgut junction in the cardia (proventriculus). Cell Cycle 10, 1109–1120. [PubMed: 21403464]

Tian A, Benchabane H, Wang Z, and Ahmed Y (2016). Regulation of stem cell proliferation and cell fate specification by Wingless/Wnt signaling gradients enriched at adult intestinal compartment boundaries. PLoS Genet. 12, e1005822. [PubMed: 26845150]

Tian A, Benchabane H, and Ahmed Y (2018). Wingless/Wnt signaling in intestinal development, homeostasis, regeneration and tumorigenesis: a Drosophila perspective. J. Dev. Biol 6, 8.

Viswanatha R, Li Z, Hu Y, and Perrimon N (2018). Pooled genome-wide CRISPR screening for basal and context-specific fitness gene essentiality in *Drosophila* cells. eLife 7, 705.

Waghmare I, and Page-McCaw A (2018). Wnt signaling in stem cell maintenance and differentiation in the Drosophila germarium. Genes (Basel) 9, 127.

Wong LL, and Adler PN (1993). Tissue polarity genes of Drosophila regulate the subcellular location for prehair initiation in pupal wing cells. J. Cell Biol 123, 209–221. [PubMed: 8408199]

Wu J, Roman A-C, Carvajal-Gonzalez JM, and Mlodzik M (2013). Wg and Wnt4 provide long-range directional input to planar cell polarity orientation in Drosophila. Nat. Cell Biol 15, 1045–1055. [PubMed: 23912125]

Yang Y, and Mlodzik M (2015). Wnt-Frizzled/planar cell polarity signaling: cellular orientation by facing the wind (Wnt). Annu. Rev. Cell Dev. Biol 31, 623–646. [PubMed: 26566118]

Yoshikawa S, McKinnon RD, Kokel M, and Thomas JB (2003). Wnt-mediated axon guidance via the Drosophila Derailed receptor. Nature 422, 583–588. [PubMed: 12660735]

Yu JJS, Maugarny-Calès A, Pelletier S, Alexandre C, Bellaiche Y, Vincent J-P, and McGough IJ (2020). Frizzled-dependent planar cell polarity without Wnt ligands. Dev. Cell, 583–592. [PubMed: 32888416]

Zirin JD, and Mann RS (2007). Nubbin and Teashirt mark barriers to clonal growth along the proximal-distal axis of the Drosophila wing. Dev. Biol 304, 745–758. [PubMed: 17313943]

Highlights

- Previous studies disagree on whether Wnt ligands affect planar cell polarity (PCP)
- Multiplex *in vivo* CRISPR or RNAi against multiple Wnt ligands does not alter PCP
- CRISPR against *wntless/evi* does not affect PCP
- We find no evidence that Wnt ligands are required for PCP in *Drosophila*

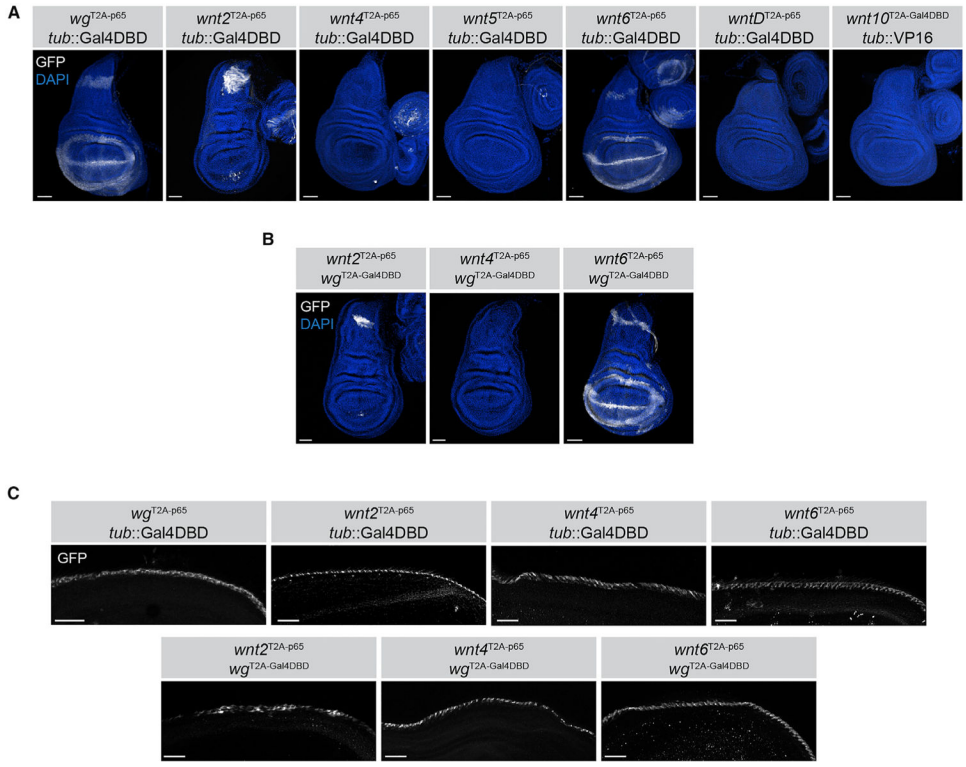

Figure 1. Analysis of Wnt Gene Expression and Co-expression Using Split-Gal4 Reporters in the Larval and Pupal Wing

(A) Expression pattern of each reporter construct, visualized by crossing to a ubiquitously expressed reciprocal split-Gal4 reporter, visualized with UAS:EGFP or UAS:EYFP (see STAR Methods).

(B) Intersection of *wg* expression domain with *wnt2, wnt4*, and *wnt6* in the L3 wing disc.

(C) Co-expression of *wg, wnt2, wnt4*, and *wnt6* in the pupal wing margin. Bottom row shows co-expression of *wg* with *wnt2, wnt4*, and *wnt6*, respectively. Portions of the anterior wing margin of ~45–60 h APF pupal wings are shown. Scale bars, 50 μm.

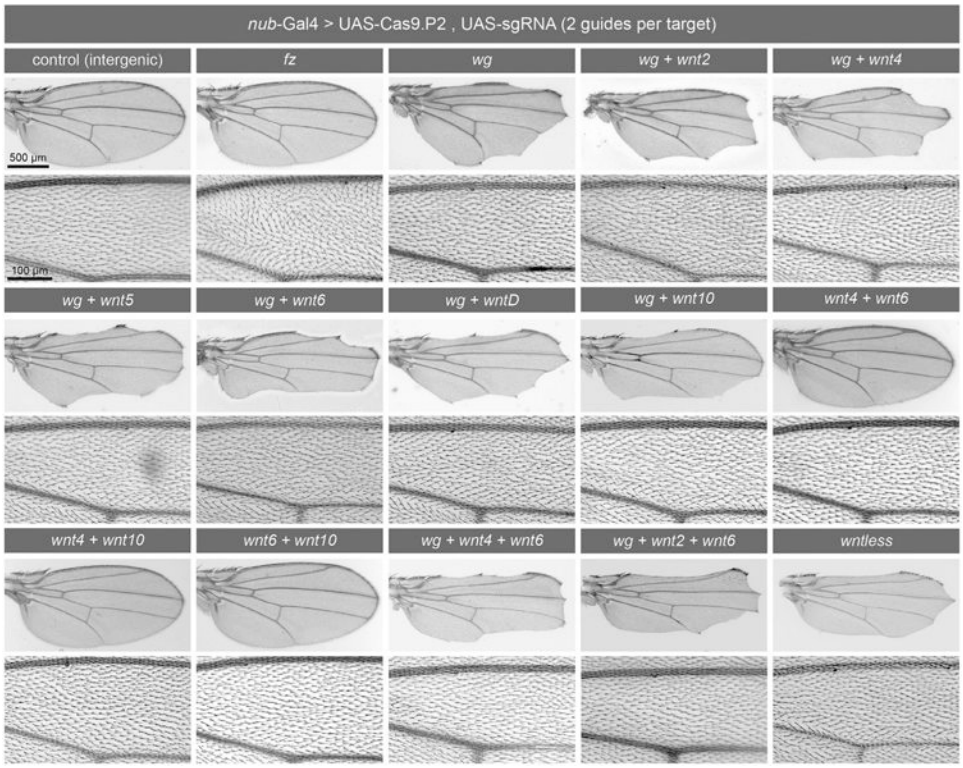

Figure 2. Multiplexed Somatic CRISPR Knockout of Wnt Genes or *wntless* Does Not Disrupt Planar Cell Polarity

UAS:sgRNAs targeting the indicated genes (two guides per target gene) were co-expressed with UAS:Cas9 in the developing wing using *nub-Gal4*. An example of a PCP phenotype is shown for *fz*. Overall wing morphology is shown in the top rows, and magnified views of wing hair orientation in the L3-L4 intervein region are shown in bottom rows; note that CRISPR against *wg* results in shorter L3-L4 intervein distance. Images are representative of approximately 20 wings analyzed per genotype.

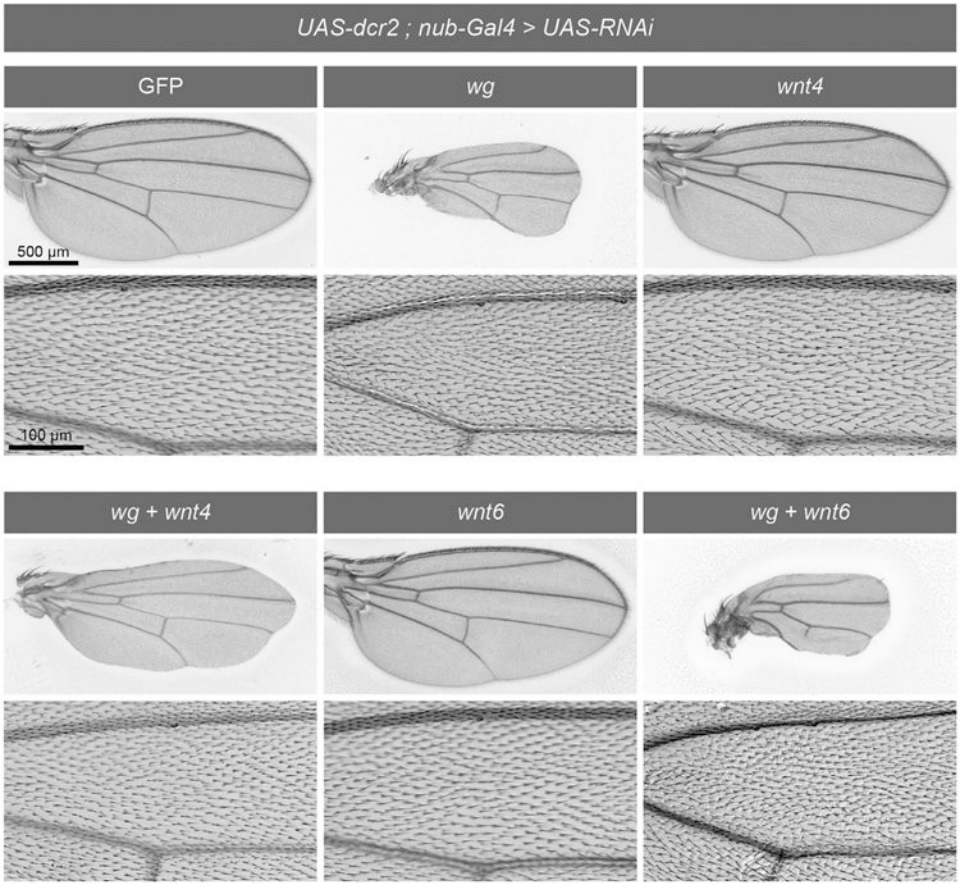

Figure 3. Pairwise Double RNAi of *wg, wnt4,* and *wnt6* Does Not Disrupt PCP Patterning in the Wing

UAS:RNAi constructs targeting the indicated genes were co-expressed with *UAS:dcr2* in the developing wing using *nub-Gal4*. Overall wing morphology is shown in the top rows, wing hair orientation in the L3-L4 intervein region is shown in magnification in the bottom rows. Images are representative of approximately 20 wings analyzed per genotype.

KEY RESOURCES TABLE

REAGENT or RESOURCE	SOURCE	IDENTIFIER
Antibodies		
Rabbit anti-GFP, Alexa 488 conjugate	Molecular Probes	(Molecular Probes Cat# A-21311, RRID:AB_221477)
Anti-Digoxigenin-AP, Fab fragments	Sigma Aldrich	(Sigma-Aldrich Cat# 11093274910, RRID:AB_2734716)
Experimental Models: Cell Lines		
Drosophila melanogaster S2R+ cells pMK33/Cas9	Perrimon lab (Viswanatha et al., 2018)	pMK33/Cas9
Experimental Models: Organisms/Strains		
Drosophila melanogaster nub-Gal4 ; UAS:Cas9.P2	Bloomington Drosophila Stock Center (BDSC)	(BDSC Cat# 67086; RRID:BDSC_67086)
Drosophila melanogaster UAS:dcr2 ; nub-Gal4	Bloomington Drosophila Stock Center (BDSC)	(BDSC Cat# 25754; RRID:BDSC_25754)
Drosophila melanogaster pnr-Gal4 / TM3	Perrimon lab stock	N/A
Drosophila melanogaster elav-Gal4 ; UAS:Cas9.P2	Bloomington Drosophila Stock Center (BDSC)	(BDSC Cat# 67073; RRID:BDSC_67073)
Drosophila melanogaster tub::Gal4DBD, UAS:EGFP	Bloomington Drosophila Stock Center (BDSC)	(BDSC Cat# 60298; RRID:BDSC_60298)
Drosophila melanogaster tub::VP16[AD], UAS:EYFP	Bloomington Drosophila Stock Center (BDSC)	(BDSC Cat# 60294; RRID:BDSC_60294)
Drosophila melanogaster wnt4 CRIMIC	Bloomington Drosophila Stock Center (BDSC)	(BDSC Cat# 67449; RRID:BDSC_67449)
Drosophila melanogaster "GTRACE" GTRACE:UAS-RedStinger, UAS-Flp1.D, Ubi (FRT.Stop)Stinger/CyO	Bloomington Drosophila Stock Center (BDSC)	(BDSC Cat# 28280; RRID:BDSC_28280)
Drosophila melanogaster GFP RNAi	Perrimon lab stock	HMS00314
Drosophila melanogaster pCFD6-wntless^{2X}	Fillip Port & Simon Bullock	N/A
Drosophila melanogaster wg RNAi	Vienna Drosophila Resource Center (VDRC)	VDRC #104579 (KK collection)
Drosophila melanogaster wnt4 RNAi	Bloomington Drosophila Stock Center (BDSC)	(BDSC Cat# 29442; RRID:BDSC_29442)
Drosophila melanogaster wnt6 RNAi	Vienna Drosophila Resource Center (VDRC)	VDRC #26669 (GD collection)
Drosophila melanogaster w ;; pCFD6-wg^{2X}	This study (see Table S1)	N/A
Drosophila melanogaster w ; pCFD6-wg^{2x}-wnt2^{2x}	This study (see Table S1)	N/A
Drosophila melanogaster w ; pCFD6-wg^{2x}-wnt4^{2x}	This study (see Table S1)	N/A
Drosophila melanogaster w ; pCFD6-wg^{2x}-wnt5^{2x}	This study (see Table S1)	N/A
Drosophila melanogaster w ; pCFD6-wg^{2x}-wnt6^{2x}	This study (see Table S1)	N/A
Drosophila melanogaster w ; pCFD6-wg^{2x}-wntD^{2x}	This study (see Table S1)	N/A
Drosophila melanogaster w ; pCFD6-wg^{2x}-wnt10^{2x}	This study (see Table S1)	N/A
Drosophila melanogaster w ; pCFD6-wnt4^{2x}-wnt6^{2x}	This study (see Table S1)	N/A
Drosophila melanogaster w ; pCFD6-wnt4^{2x}-wnt10^{2x}	This study (see Table S1)	N/A
Drosophila melanogaster w ; pCFD6-wnt6^{2x}-wnt10^{2x}	This study (see Table S1)	N/A
Drosophila melanogaster w ; pCFD6-wnt4^{2x}-wnt6^{2x} ; pCFD6-wg^{2x}	This study (see Table S1)	N/A
Drosophila melanogaster w ; pCFD6-wnt2^{2x}-wnt6^{2x} ; pCFD6-wg^{2x}	This study (see Table S1)	N/A

REAGENT or RESOURCE	SOURCE	IDENTIFIER
Drosophila melanogaster w ; pCFD6-intergenic control	This study (see Table S1)	N/A
Drosophila melanogaster w ; pCFD6-fz	This study (see Table S1)	N/A
Drosophila melanogaster yv ; pCFD4FLPOUT-fz	This study (see Table S1)	N/A
Drosophila melanogaster yv ; pCFD4FLPOUT-fz2	This study (see Table S1)	N/A
Drosophila melanogaster yv ; pCFD4FLPOUT-fz3	This study (see Table S1)	N/A
Drosophila melanogaster yv ; pCFD4FLPOUT-fz4	This study (see Table S1)	N/A
Drosophila melanogaster yv ; pCFD4FLPOUT-fz-fz2	This study (see Table S1)	N/A
Drosophila melanogaster yv ; pCFD4FLPOUT-fz-fz3	This study (see Table S1)	N/A
Drosophila melanogaster yv ; pCFD4FLPOUT-fz-fz4	This study (see Table S1)	N/A
Drosophila melanogaster yv ; pCFD4FLPOUT-fz2-fz3	This study (see Table S1)	N/A
Drosophila melanogaster yv ; pCFD4FLPOUT-fz2-fz4	This study (see Table S1)	N/A
Drosophila melanogaster yv ; pCFD4FLPOUT-fz3-fz4	This study (see Table S1)	N/A
Drosophila melanogaster wgT2A-p65	This study (see Table S1)	N/A
Drosophila melanogaster wnt2T2A-p65	This study (see Table S1)	N/A
Drosophila melanogaster wnt4T2A-p65	This study (see Table S1)	N/A
Drosophila melanogaster y v wnt5T2A-p65	This study (see Table S1)	N/A
Drosophila melanogaster wnt6T2A-p65	This study (see Table S1)	N/A
Drosophila melanogaster wntDT2A-p65	This study (see Table S1)	N/A
Drosophila melanogaster wnt10T2A-Gal4DBD	This study (see Table S1)	N/A
Drosophila melanogaster wgT2A-Gal4DBD	This study (see Table S1)	N/A
Drosophila melanogaster UAS:^{2x}EGFP	Bloomington Drosophila Stock Center (BDSC)	(BDSC Cat# 60293; RRID:BDSC_60293)
Drosophila melanogaster wnt4T2A-Gal4	This study (see Table S1)	N/A
Oligonucleotides		
PCR primers	See Table S2	
In situ RNA probes	See Table S2	
Recombinant DNA		
pCFD6	Addgene	73915
pBPp65ADZpUw (split-Gal4 p65)	Addgene	26234
pBPZpGAL4DBDUw (split-Gal4 Gal4DBD)	Addgene	26233
pHD-dsRed-attP	Addgene	51019
pCFD4FLPOUT	This study	N/A
Software and Algorithms		
Zen	www.zeiss.com	(ZEN Digital Imaging for Light Microscopy; RRID:SCR_013672)
Adobe Photoshop vCS6	www.adobe.com	(Adobe Photoshop; RRID:SCR_014199)
Adobe Illustrator V23.0.4	www.adobe.com	Adobe Illustrator; RRID:SCR_010279
Helicon Focus	www.heliconsoft.com	(Helicon Focus; RRID:SCR_014462)